



ELSEVIER

Contents lists available at ScienceDirect

Biosensors and Bioelectronics

journal homepage: www.elsevier.com/locate/bios

High sensitivity automated multiplexed immunoassays using photonic crystal enhanced fluorescence microfluidic system



Yafang Tan^a, Tiantian Tang^a, Haisheng Xu^b, Chenqi Zhu^a, Brian T. Cunningham^{a,c,*}

^a Department of Electrical and Computer Engineering, University of Illinois at Urbana-Champaign, 208 North Wright Street, Urbana, IL 61801, USA

^b Department of Material Science, University of Illinois at Urbana-Champaign, 208 North Wright Street, Urbana, IL 61801, USA

^c Department of Bioengineering, University of Illinois at Urbana-Champaign, 208 North Wright Street, Urbana, IL 61801, USA

ARTICLE INFO

Article history:

Received 6 April 2015

Received in revised form

14 May 2015

Accepted 17 May 2015

Available online 19 May 2015

ABSTRACT

We demonstrate a platform that integrates photonic crystal enhanced fluorescence (PCEF) detection of a surface-based microspot fluorescent assay with a microfluidic cartridge to achieve simultaneous goals of high analytic sensitivity (single digit pg/mL), high selectivity, low sample volume, and assay automation. The PC surface, designed to provide optical resonances for the excitation wavelength and emission wavelength of Cyanines 5 (Cy5), was used to amplify the fluorescence signal intensity measured from a multiplexed biomarker microarray. The assay system is comprised of a plastic microfluidic cartridge for holding the PC and an assay automation system that provides a leak-free fluid interface during introduction of a sequence of fluids under computer control. Through the use of the assay automation system and the PC embedded within the microfluidic cartridge, we demonstrate pg/mL-level limits of detection by performing representative biomarker assays for interleukin 3 (IL3) and Tumor Necrosis Factor (TNF- α). The results are consistent with limits of detection achieved without the use of the microfluidic device with the exception that coefficients of variability from spot-to-spot are substantially lower than those obtained by performing assays with manual manipulation of assay liquids. The system's capabilities are compatible with the goal of diagnostic instruments for point-of-care settings.

© 2015 Elsevier B.V. All rights reserved.

1. Introduction

As molecular diagnostics are increasingly utilized as a minimally invasive tool for determining the health status of patients and for guiding the course of therapy, there is intense interest in transitioning central laboratory-based tests towards the point-of-care through assays that can be performed easily within health clinics. There is also a drive towards gaining a more comprehensive view of a patient's health status from a single specimen through multiplexed tests that are capable of determining the presence and concentration of many analytes simultaneously. The ability to perform such testing using only a single droplet of serum would aid in the widespread acceptance of such tests, particularly if a sample could be gathered by a finger-stick, rather than drawing blood by a highly skilled phlebotomist. For example, rapid detection of immune-related biomarkers (i.e. specific antibodies) to pathogenic antigens, tumor antigens, or allergenic antigens is an important aspect of allergy characterization and diagnosis of

autoimmune disease (Robinson et al., 2002; Wong et al., 2009; Debnath, 2010). Detection of soluble protein biomarkers is used heavily in oncology for early detection of several forms of cancer (Ward et al., 2006; Nam et al., 2003; Tannapfel et al., 2003; Patz et al., 2007; Zhang et al., 2004; Luo et al., 2003; Diamandis et al., 2003a, b; Maurya et al., 2007), cardiovascular disease (Vasan, 2006; Wang et al., 2006), neurological disorders and infectious disease, as disease specific biomarker panels continue to be discovered and validated by clinical studies (Jain, 2010). New types of biomarkers are the subject of intense research interest, including circulating tumor DNA (ctDNA) (Bettegowda et al., 2014; Dawson et al., 2013; Newman et al., 2014), and microRNA (miRNA) biomarkers for cancer (Khoo et al., 2012; Jeffrey, 2008; Sita-Lumsden et al., 2013). The concept of a "liquid biopsy" is gaining acceptance as an approach for assessing many aspects of a patient's health without expensive medical imaging technology, exposure to ionizing radiation, or extraction of tissue from the patient. When implemented with a sensitive, inexpensive, rapid, and multiplexed detection technology, a liquid biopsy may serve as a primary form of health assessment, early disease detection, and treatment-tracking approach that will complement more invasive and expensive diagnostic modalities.

A key unmet need for soluble biomarker detection for

* Corresponding author at: Department of Electrical and Computer Engineering, University of Illinois at Urbana-Champaign, 208 North Wright Street, Urbana, IL 61801, USA.

E-mail address: bcunning@illinois.edu (B.T. Cunningham).

achieving clinical relevance is improved sensitivity. Early diagnostic applications for cancer, for example, require detection of biomarkers that are produced by, or in response to, a small number of cells. The biomarker is diluted throughout the volume of blood within a person, so that when a sample of peripheral blood is drawn, the biomarker concentration can be $<1\text{--}10$ pg/mL. (For reference, 1 pg/mL of a typical cytokine such as IL-6 is equivalent to ~ 45 fM. A 10 μL sample at this concentration contains 0.45 attomoles of IL-6.) In addition to high sensitivity, clinical diagnostic laboratories require automated platforms that can perform rapid multiplexed biomarker analysis at low cost/assay and that can quantify small changes in concentration. Consensus is emerging that multiple, mutually exclusive biomarkers in an assay will lead to better clinical management of disease, compared to assessment of a single biomarker, and will allow subtle differences in patient populations (gender, race, age) to be understood (Neagu et al., 2011; Gonzalez et al., 2011; Zangar et al., 2005).

Among the current methodologies of biomarker detection, sandwich antibody microarrays hold great potential due to their demonstrated capacity to detect analytes at <10 pg/mL concentration in complex media (such as serum) (Robinson et al., 2002; Fan et al., 2008) with the use of only 3–10 μL samples, no assay cross-reactivity, and fast binding kinetics. Using a photonic crystal (PC) surface to enhance the fluorescence output from a biomarker microarray, we have previously published the results of studies that successfully achieved high sensitivity for multiplexed cancer biomarker detection (Huang et al., 2011; George et al., 2013; Ganesh et al., 2007; Pokhriyal et al., 2010). More recently, we developed a high sensitivity, compact, and inexpensive detection platform for Photonic Crystal Enhanced Fluorescence (PCEF) that uses a silicon-based PC surface and a compact/inexpensive laser line-scanning detection instrument in an effort to maximize the coupling efficiency of light into the PC structure (George et al., 2013). Our previous work demonstrates clearly that PCEF surfaces can be inexpensively mass-manufactured from silicon wafers using conventional processes used in integrated circuit manufacturing, and that silicon-based PCs do not introduce background fluorescence (which is also amplified by PCEF), thus enabling detection of biomarkers present at low concentrations.

Our previously-demonstrated application of PCEF for multiplexed, high sensitivity detection of soluble protein and miRNA biomarkers was performed as a proof-of-principle using an assay protocol that required a highly skilled person to introduce all reagents and to perform all assay wash steps manually using a pipette. For this approach, a relatively large (1×0.5 in.²) silicon-based PC chip was fitted with a silicone rubber gasket with a screw-on metal holding fixture that would enable the operator to define up to ten distinct assay wells upon the PC surface. Micro-spot fluorescent immunoassays for TNF- α and IL-3 performed on this platform demonstrated that the system can achieve pg/mL-level sensitivity. Although only a 10 μL sample was consumed with the use of 2 mm-diameter wells, manual sample handling presented difficulties in injecting liquid and required dedicated time/labor. The performance and implementation characteristics of performing PCEF microarray assays with manual liquid sample handling greatly limits its scalability and accessibility to clinicians, including a disjointed workflow that required manual intervention across multiple steps and used the PC surface area inefficiently. Therefore, the development of a simpler and automatic format is desired to move PCEF-based biomarker assays closer to clinical applications such as point-of-care diagnostics.

In this paper, we present a new platform that combines PCEF and microfluidic sample handling to achieve high analytic sensitivity (1.57 pg/ml), high selectivity, low sample volume, and assay automation. The novel elements of the present work include the

design and fabrication of a low-cost PC-integrated microfluidic cartridge that incorporates a stereolithographic 3D printed cartridge body (Melchels et al., 2010; Zhang et al., 2012; Au et al., 2014) a laser-cut fluidic channel (Choudhury and Shirley, 2010; Eltawahni et al., 2012; Nie et al., 2013) a low autofluorescent transparent glass viewing window, and a substantially smaller (2×8 mm²) PC chip. The function of the cartridge is to hold the PC in place during the assay, to provide a leak-free and simple-to-operate interface to an external assay automation system, and to provide a stable mechanical platform during fluorescence scanning. The assay automation system introduces the correct sequence of fluids through the cartridge from a set of liquid reservoirs (external to the cartridge) under computer control. Here we demonstrate the first use of the cartridge and assay automation system for two representative biomarker assays in the form of a small sandwich antigen microarray. While substantially reducing the operator time and complexity required to perform an assay, we demonstrate that achieved limits of detection are equivalent to those obtained with the more “manual” approach, while the use of microfluidic flow (rather than pipette-based liquid handling) was found to significantly improve the spot-to-spot reproducibility of the assay. We found that the coefficients of variability across spots were decreased most dramatically for the lowest concentration assays.

2. Materials and methods

2.1. Design and fabrication of a PC-embedded microfluidic device

The PC is comprised of a periodic surface structure fabricated with a low refractive index (RI) silicon dioxide (SiO₂, RI=1.46) layer on a silicon substrate (George et al., 2013). The grating structure is coated with a high RI titanium dioxide (TiO₂, RI=2.35) thin film. The PC has a period of 360 nm, a duty cycle of 36%, a grating depth of 40 nm, and a TiO₂ thickness of 130 nm. A commercial vendor (Novati Technologies Inc., Austin TX) was contracted for performing photolithography and reactive ion etching (RIE) of the SiO₂ grating structure over 8-inch diameter wafers, while TiO₂ thin films were deposited upon whole wafers at a second vendor (Intlvac Inc., Niagara Falls NY). Following lithography, etching, and TiO₂ deposition, the wafers were diced into 2×8 mm² pieces. An SEM image showing the surface structure of the PC is presented in the inset of Fig. 1(c).

As shown in Fig. 1(a), the cartridge assembly is comprised of a 3D printed plastic base with inlet/outlet through-holes, a Double-Sided Adhesive (DSA) fluid channel, and a nonfluorescent glass coverslip. The plastic base was designed by three-dimensional (3D) design software (PTC Creo Parametric 2.0) and fabricated by stereolithography of optically clear resin (WaterClear Ultra 10122) using a Viper SLA System. The base layer is 75 mm long, 25 mm wide, 6 mm thick, and incorporates a recessed region ($2.2 \text{ mm} \times 8.2 \text{ mm}$), into which the PC chip of the same dimension was attached by adhesive. The middle layer is comprised of DSA (3MTM Optically Clear Adhesive 8212) with a $\sim 2 \times 12$ mm² wide and 150 μm deep channel in the center, aligned with the fluid inlet/outlets and the PC. In order to ensure device cleanliness, non-contact laser cutting was used to cut the channel area on the DSA. The bottom layer is a thin transparent coverslip, which allows a video camera to monitor the flow inside the channel during the assay, and subsequently for the laser scanning instrument to illuminate the microarray spots for fluorophore excitation. Shott Glass (#1098576, $24 \times 60 \times 0.17$ mm³) was chosen for its tight thickness tolerance, which minimizes spherical aberration, and its low background fluorescence, therefore promoting high quality images of the fluorescence signal during scanning. The three layers

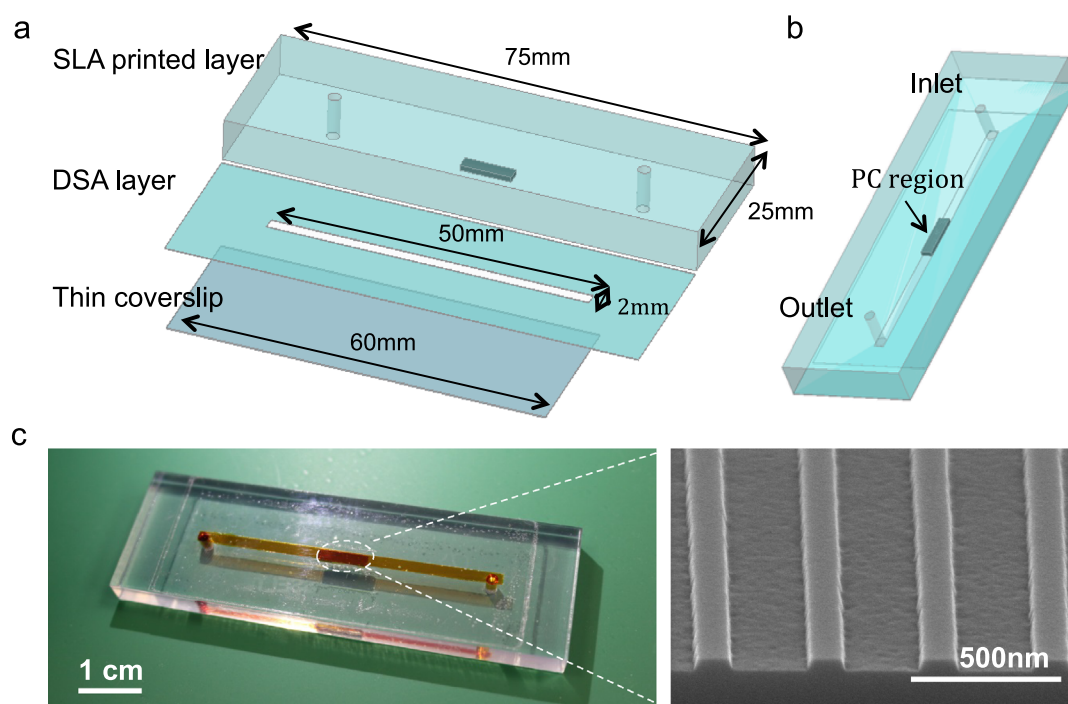


Fig. 1. Schematics of the PC microfluidic cartridge (a) before and (b) after assembly, comprised of a plastic base, Double-Sided Adhesive (DSA) and a nonfluorescent glass coverslip. The plastic base incorporates a recessed region into which the PC chip of the same dimension is attached with adhesive. The DSA layer contains a laser-cut slot that corresponds to the walls of the microfluidic channel, and is sandwiched between the coverslip and the base. The transparent window enables a camera to monitor the flow inside the channel during the assay process, and provides access to laser excitation of the fluorophores during the detection step. (c) Left: a photo of a fabricated microfluidic chip in which red food dye was introduced throughout the inlet; Right: SEM of the PC surface. (For interpretation of the references to color in this figure legend, the reader is referred to the web version of this article.)

were joined by the DSA layer in a custom-built mechanical alignment fixture and pressed by a roller at room temperature to seal them together. Room temperature sealing of the chip is desired, so as to not damage protein-based capture molecules that are printed upon the PC before final cartridge assembly. Fig. 1 (c) shows a photo of a fabricated microfluidic chip in which red food dye was introduced through the inlet.

2.2. Computer-controlled microfluidic system

Using components shown in Fig. 2(a), the entire assay process was automated with no intervention from the user other than introduction of a droplet of test sample into the inlet reservoir (volume $\sim 10 \mu\text{L}$). A 3-to-1 valve (Cole-Parmer Manifold Mixing Solenoid Valve) introduces either compressed nitrogen, buffer solution, or Cy5-labeled detection antibody into the channel. The assay liquids are stored in 2 mL reservoirs, as they are common to all assays that will be performed by the instrument, and are pushed from the reservoir to the cartridge by pneumatic pressure. The fluid selection is determined by a programmable microfluidic controller (FlowTest™ Programmable Microfluidic Controller). The fluid driving force was supplied by compressed nitrogen, which was regulated by a pressure controller (Fluigent MFCS-EZ) that provided pulseless and highly stable ($< 0.1\%$ CV) flows. A digital camera (Dino-Lite AM3111T) located beneath the fixture monitored the flow through a hole in the fixture. Under computer control, the system regulates the fluid flow rate, while enabling real-time monitoring of the exposure status of the PC by an integrated video camera.

To ensure leak-proof sealing and zero dead volume, flanged end tubes and a custom-machined metal frame were used in our system (Wilhelm et al., 2013). The seal was based on a forced fit between the flanged ends of chemically inert polytetrafluoroethylene (Cole-Parmer PTFE EW-06605-27 1/16") tubing and

the flat outer surface of the microfluidic cartridge. The flange was created by heating the end of the tubing and pressing it against a metal washer (Wilhelm et al., 2013). The metal frame maintains alignment between the tubing and the inlet/outlets of the microfluidic chip, while screws between the upper and lower metal holding plates of the fixture apply sufficient pressure for a leak-proof seal. A schematic of the sealing fixture is shown in Fig. 2(b).

2.3. Immunoassay procedure using microfluidic sample handling

To demonstrate the capability of the microfluidic system, microspot immunoassays for two cytokines (interleukin 3 (IL-3) and tumor necrosis factor alpha (TNF- α)) were performed using PCs embedded in the cartridge. Before printing spots, the PC surface was cleaned and activated with a vapor-phase epoxysilane process. The epoxysilane chemistry was chosen for its low background fluorescence (Dorvel et al., 2009) and high binding capacity for antibody molecules (Zhu et al., 2000). The devices were first cleaned by sonication in 2" petri dishes of acetone, isopropanol, and deionized (DI) water for 2 min each. The devices were then dried in a stream of N_2 and then treated in an oxygen plasma system (Diener, Pico) for 10 min (power of 100 W, pressure of 0.75 mTorr). The backside of each device was then adhered to the inside of a screw top lid of a 2" glass container. At the base of the container, 100 μL of (3-Glycidoxypropyl) trimethoxysilane (GPTS, Sigma Aldrich, Saint Louis, MO) was placed and the lid was securely placed over the dish. After securely tightening the lids, each dish with a device adhered to its lid was placed in a vacuum oven for an overnight incubation at a temperature of 80 $^\circ\text{C}$ and a pressure of 30 Torr. The devices were then detached from the lids and sonicated in 2" petri dishes of toluene, methanol, and DI water for 2 min each and dried under a stream of N_2 .

After silanization, the protein arrays were printed onto the PC surface. A PC holds two subarrays, and each subarray contains

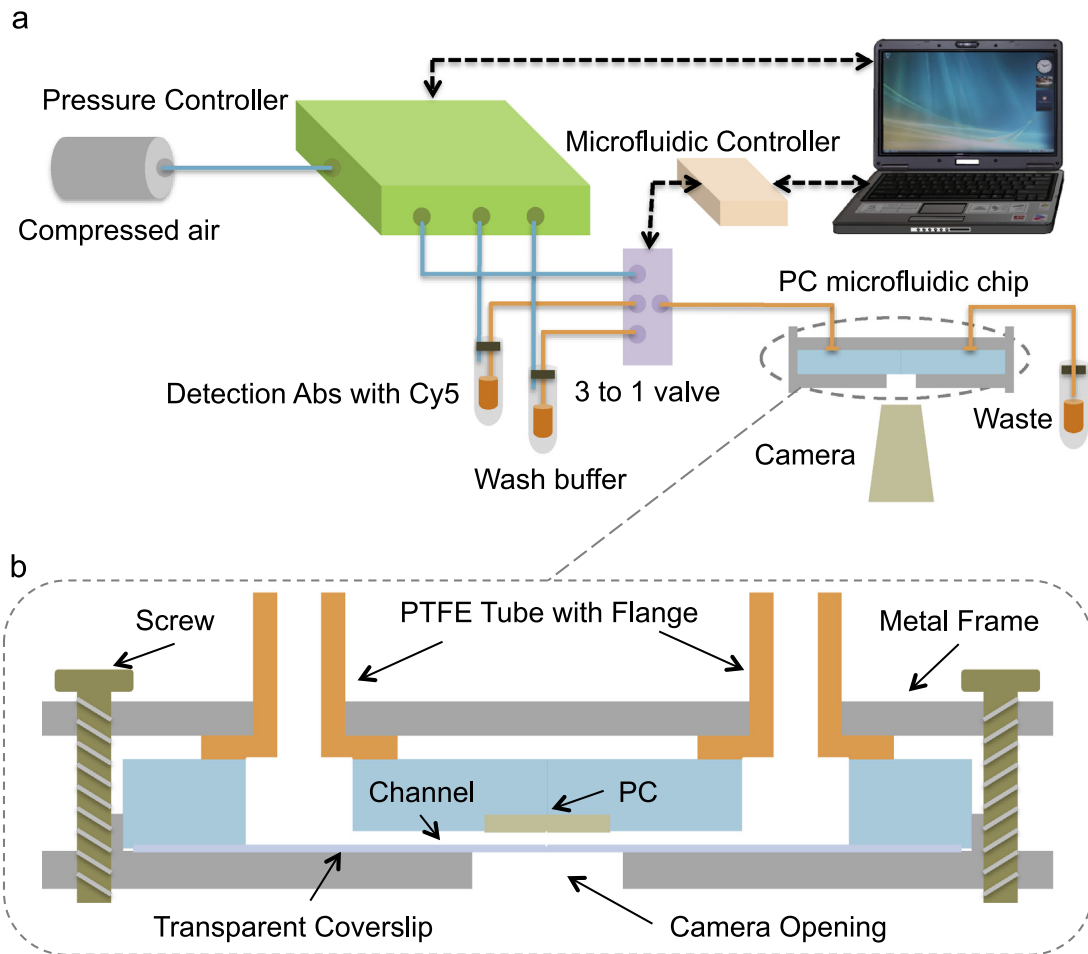


Fig. 2. (a) Schematic drawing of the microfluidic control system. A 3-way valve enables computer-controlled selection of compressed nitrogen, buffer solution, or Cy5-tagged detection antibodies into the chip inlet port. Fluid driving force is supplied by compressed nitrogen for pulseless and highly stable flows, while a digital camera enables real-time monitoring of the liquid in contact with the PC. (b) Schematic of the leak-proof seal between the microfluidic inlet/outlet holes and the assay automation instrument. The seal utilizes a force fit between flanged ends of chemically inert tubing and the flat outer surface of the microfluidic cartridge.

4 sets of 4 replicate spots for each protein, resulting in an array with 16 spots. The first row is a fluorescent-tagged protein for array orientation/location (Alexa-Fluor-555 fluorescent streptavidin conjugates, Life Technologies), the second row is the TNF- α antibody (R&D systems Inc.), the third row is a negative control of Phosphate Buffered Saline (PBS) (pH=7.4), and the last row is the IL-3 antibody (R&D systems Inc.). The antibody microarrays on the PC were printed by a desktop nanofabrication system (Arrayit NanoPrint LM60 Microarrayer) while the chip was in a free format (i.e. not yet attached to the cartridge base). The printing was performed under a controlled environment using an environmental chamber (ambient temperature and 50% relative humidity). Four pins (946MP3 Microarray Printing Pins) were used to print the two antibodies at a concentration of 1 mg/mL, which results in 5×10^9 molecules/mm². The binding affinity is ~ 50 nM for TNF-alpha antibody while ~ 1 nM for IL3 antibody (Borras and Tietz, 2010). The positive control was printed at a protein concentration of 10 μ g/mL, and the negative control was comprised of printed buffer solution. Printing pins were cleaned between sample pickups with 15 s sonication and 4 cycles of washing (2.5 s) and drying (1 s). Measured spot diameters were 79 ± 2 μ m. Row spacing was 149 ± 3 μ m and column spacing was 200 ± 0.8 μ m. The printed substrates were incubated in a sealed box with a desiccant overnight at ambient temperature. Next, the arrays were blocked with casein blocking buffer (BioRad, Hercules, CA) for 1 h before they were washed three times with 0.02% (v/v) tween 20 in PBS (PBST). The substrates were then dried and put in a sealed box

for future use.

Following array printing and surface blocking, a PC substrate with antibody microspots was glued into the recess of the plastic base of the cartridge. Next, the glass cover slip was bonded to the base using the laser-patterned DSA film to complete the fabrication process. Each completed microfluidic cartridge was used to perform one immunoassay for one mixture of different antigen concentrations in casein buffer. One thing to be noted is that 50 chips were printed with microarrays and assembled into a microfluidic channel one time, in order to help users avoid the spotting and assembly steps and directly run the automatic assay every time. Since the antibody microarrays can be stored in freezer at dry environment for more than six months, the quality of the microfluidic chips are not effected by the storage. 10 μ L of test sample, comprised of a mixture of TNF- α and IL-3 in PBS was introduced into the microchannel inlet by a pipette. The hydrophilic nature of the inner channel surface facilitates liquid flow into the channel by capillary action, so the droplet of test sample covers the PC array without any intervention from the user or application of external fluid driving force. The cytokine TNF- α (R&D systems Inc.) was assayed at the following seven concentrations: 1 ng/mL, 0.25 ng/mL, 62.50 pg/mL, 15.62 pg/mL, 7.8 pg/mL, 3.9 pg/mL, and 1.9 pg/mL. The concentration of IL-3 (R&D systems Inc.) is 10 times higher than that of TNF- α in all assayed antigen mixtures. After a 3-hour incubation of the test sample with the microarray, the cartridge was loaded into the assay automation system, to perform the washing and labeling steps of the assay. The device was

washed by flowing PBST for 1 min with an applied pressure of 25 mBar to remove the unreacted antigens. Next, the 1 $\mu\text{g}/\text{mL}$ fluorescent-labeled secondary antibody mixture (Alexa Fluor[®] 647 TNF- α antibody and Alexa Fluor[®] 647 IL-3 antibody, at the mixing ratio of 1:1, Novus Biologicals, LLC) was introduced into the microchannel with an applied pressure of 25 mBar for 30 s. After 1 h incubation, the microchannel was washed again by flowing PBST for 1 min to remove the unreacted fluorescent-labeled secondary antibody solution. Finally, an air flow was produced in the microchannel by applying high-pressure nitrogen gas (345 mBar) to the inlet to remove remaining liquid. The PC surface was completely cleaned and dried in 10 s due to its hydrophobicity, as observed by the imaging camera. Following the immunoassay process, the microfluidic chip was removed from the automation system and transferred to the PCEF laser scanning instrument for fluorescent imaging.

2.4. PCEF scanner and image acquisition

We have designed and constructed a PCEF microarray detection instrument that provides collimated illumination and the ability to tune the incident angle to precisely match the resonant coupling condition (Block et al., 2009) while focusing the light from a fiber-coupled semiconductor laser to a 8 μm line with a cylindrical lens (Chaudhery et al., 2012). The purpose of the custom detection instrument is to optimize coupling of laser illumination to the PC surface. As described in previously published reports (Block et al., 2009; Chaudhery et al., 2012), the excitation laser is collimated in the plane perpendicular to the grating lines, but focused in the plane parallel to the grating (Fig. 3). Collimated light with electric field polarization perpendicular to the grating lines is able to couple most efficiently with the PC resonant mode, but the light need only be collimated with respect to a single axis. Along the orthogonal axis, light can be focused without compromising coupling efficiency to the PC, and thus focus along one axis is used to achieve high illumination intensity. The system is designed for optimal interaction with the PC for both enhanced excitation and enhanced extraction, using design principles discussed, modeled, and demonstrated in (George et al., 2013). The focal point of the cylindrical lens is located at the back focal plane of the objective. Linear translation of the cylindrical lens by a computer-controlled motion stage results in adjustment of the incident angle to achieve the 'on resonance' illumination. A semiconductor laser diode (Al-GaAs, 70 mW, $\lambda=637$ nm) is expanded to a diameter of 1 mm, and focused to an 8 μm wide line onto the PC surface by a cylindrical lens. A mirror coupled to a computer-controlled linear translation stage enables adjustment of the incident angle from 0–20° with 0.01° increments. The grating lines of the PC are oriented perpendicular to the scan line, allowing the laser (polarized output perpendicular to the grating) designed to excite the Transverse Magnetic (TM) mode of the PC.

Using the scanner described above, a fluorescent image of the PC surface was obtained by adjusting the incident angle of the laser illumination line upon a region of the PC adjacent to the microspots and then translating the PC holding stage in increments of 2 μm past the array region, gathering a fluorescent intensity image of the line for each motion increment. Then, the fluorescent intensities of each line were assembled into a two-dimensional image of fluorescence intensity on the PC surface through a custom-built C# user interface. Spot segmentation and intensity calculations of the constructed fluorescence images were performed using ImageJ. Net spot intensity was calculated as the local background subtracted spot intensity where the local background is an annular region around a given spot. Spot signal-to-noise ratio (SNR) was calculated as the local background subtracted spot intensity divided by the standard deviation of the

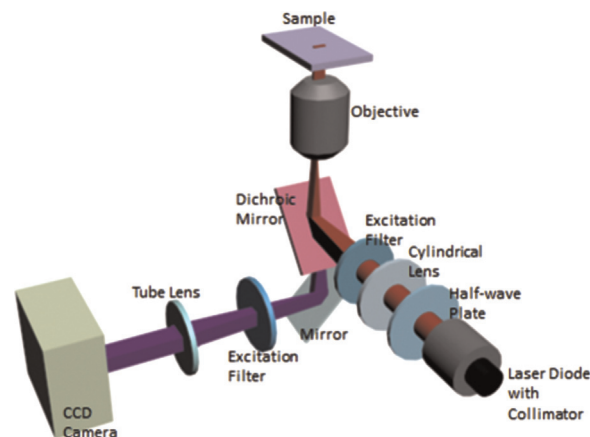


Fig. 3. Schematic diagram of the objective-coupled, line-scanning instrument used to acquire fluorescence data at the precise PC resonant angle. Equipped with a solid-state laser diode, the instrument illuminates the PC with a beam of light that is focused in one plane for high illumination intensity, but collimated in the other plane for optimally coupling the incident light to the PC resonant mode.

local background.

3. Results and discussions

3.1. Raw fluorescent intensity

Because all previous PCEF measurements of biomarker microarrays were gathered with PCs not packaged within a cartridge, we first sought to determine whether laser scanning through the glass window would have a detrimental effect on the spatial resolution, intensity, or background levels of the array. To investigate the potential effects of scanning the array through the glass window, we performed the immunoassay for 1.9 pg/mL TNF α using the PC-embedded cartridge, and then scanned the microarrays before and after removing the glass window. The illumination angle (incident angle=4.12°) and camera settings (sensitivity gain=25, exposure time=40 ms) were the same for both scans. Although we scanned the same area twice, the intensity decay due to photobleaching after the first scan is less than 0.001% (Chaudhery et al., 2011) and can be safely ignored, as the laser only illuminated the area for 120 ms, given that the exposure time of the camera was 40 ms and oversampling rate was 3. Fluorescence intensities of each micro-spot and its surrounding background were obtained by quantifying fluorescent images (Fig. 4(a)), and subsequently averaged over the four replicates. Interestingly, the spot intensity obtained by scanning through the glass window (the first red bar in Fig. 4(b)) is 20% higher than that obtained without the window (the first black bar in Fig. 4(b)). The increased intensity was attributed to the fluorescence from a small amount of fluorescently labeled secondary antibody that was absorbed onto the glass during the assay procedure. We can confirm this assumption by examining the average background intensity, which decreased from 2236 counts to 1744 counts by removing the glass (Fig. 4(b)). Net intensity was calculated as the background subtracted spot intensity, through which any fluorescence from the glass was removed. In contrast to the increase in the average spot intensity and background intensity, the average net intensity decreased to 93% if spots were scanned through the glass (the third bars in Fig. 4(b)). This small signal loss is attributed to partial light reflection at the interface between air and glass. Given that refractive index is $n_1=1.00$ for air and $n_2=1.50$ for glass, the transmittance of the fluorescence after passing the upper surface of glass is 96%, calculated by the equation:

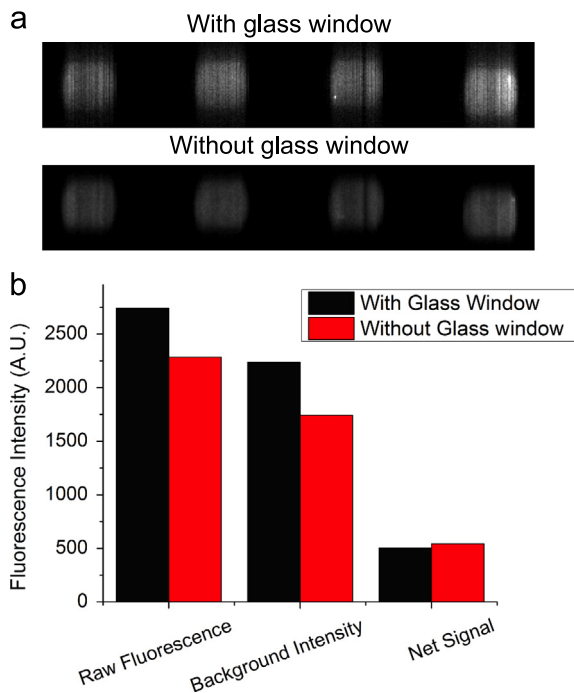


Fig. 4. (a) Fluorescent images obtained by scanning a microarray assayed with a 1.9 pg/mL TNF-sample before (the upper row) and after (the bottom row) removing the glass window. (b) Average fluorescent intensities over four replicates with (black bar) and without (red bar) glass window. Although the spot intensity obtained with a glass window is higher, the net fluorescent intensity is 6.77% lower compared to that without a glass window. (For interpretation of the references to color in this figure legend, the reader is referred to the web version of this article.)

$$T = 1 - \left(\frac{n_1 - n_2}{n_1 + n_2} \right)^2$$

Ignoring the phenomena of multiple internal reflection in the glass, transmittance of the fluorescence through the glass, adding the signal loss at the second surface, is 92%, which is close to the percentage of the signal we obtained in the experiment. Considering the small thickness and good flatness of the glass, any

absorption or scattering can be neglected. Although there was a slight decrease in the net fluorescence signal, the fluorescent spots were still distinguishable from the background, even for the assay with the lowest concentration.

3.2. Fluorescence enhancement of a PC-embedded cartridge

The PC is designed to increase the fluorescence intensity of Cy5 dyes through the enhanced excitation and extraction mechanism described previously. The enhanced extraction effect is always present, regardless of the illumination conditions. In a previous report (Huang et al., 2011), we demonstrated that enhanced extraction resulted in an approximately 5-fold increase in fluorescence intensity compared to detection on unpatterned glass. The effect of enhanced excitation can be determined by comparing the fluorescence output under the following two conditions: (a) when the incident angle of the excitation laser was adjusted to illuminate the PC at the resonant angle ('on resonance'), and (b) when the angle of incidence was selected not to coincide with the resonant coupling condition ('off resonance'). Although fluorescence enhancement by a silicon PC has been demonstrated previously (George et al., 2013), it is still necessary to characterize the enhancement factor and show that the same enhancement can be observed using a PC embedded in a microfluidic device that is covered by a glass window. In the experiment to characterize the enhanced excitation of the PC in the microfluidic device, 0.15 ng/mL of IL-3 was assayed, and the microspots were scanned at both on- and off-resonance conditions. First, the reflection spectrum of the PC (Fig. 5(c)) was acquired by illuminating the surface over a range of incident angles at the fixed excitation wavelength $\lambda=637$ nm. The on-resonance angle of illumination was 4.12° , as indicated in the spectrum, while the off-resonance angle was chosen to be 3.00° . The fluorescent images shown in Fig. 5(a) and (b) were obtained at on- and off-resonance conditions, respectively. Because of the low fluorescence at the off-resonance condition, exposure time of the camera was set to be 400 ms, 10 times higher than that of the on-resonance condition. Therefore, the on-resonance value was multiplied by a factor of 10 before direct comparison to the off-resonance value. It can be observed in Fig. 5(d) that by scanning the PC at its resonant angle,

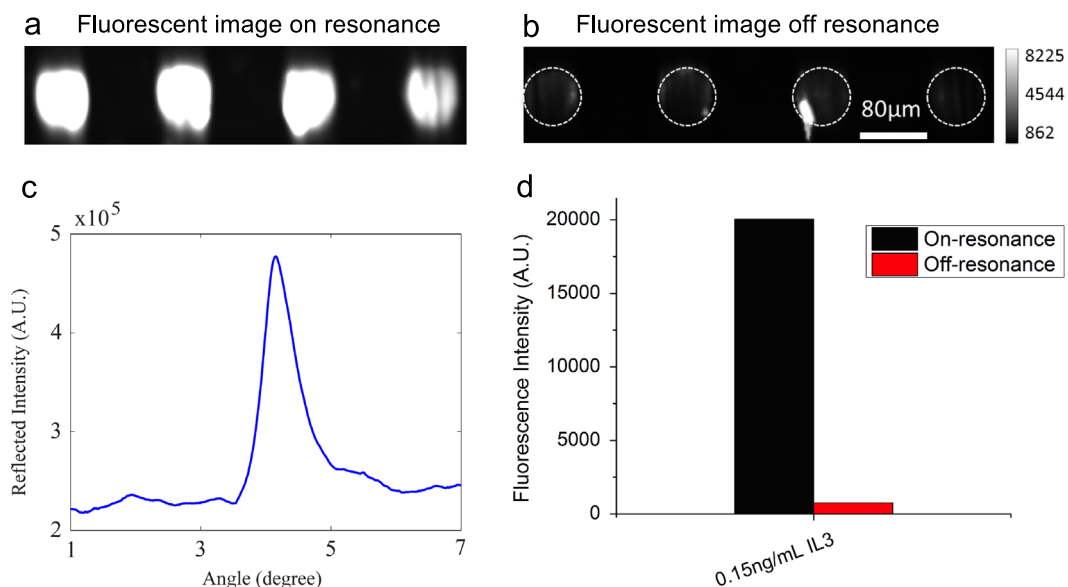


Fig. 5. (a) Fluorescent images obtained at (a) on-resonance and (b) off-resonance illumination conditions. (c) Reflection spectrum of the PC acquired by illuminating the surface over a range of incident angles at the fixed excitation wavelength $\lambda=637$ nm. (d) Average fluorescent intensities when the PC embedded in microfluidic channel were on resonance (black bar) and off resonance (red bar). The on-resonance intensity was multiplied by a factor of 10 in order to compensate for shorter exposure time compared to off-resonance condition. (For interpretation of the references to color in this figure legend, the reader is referred to the web version of this article.)

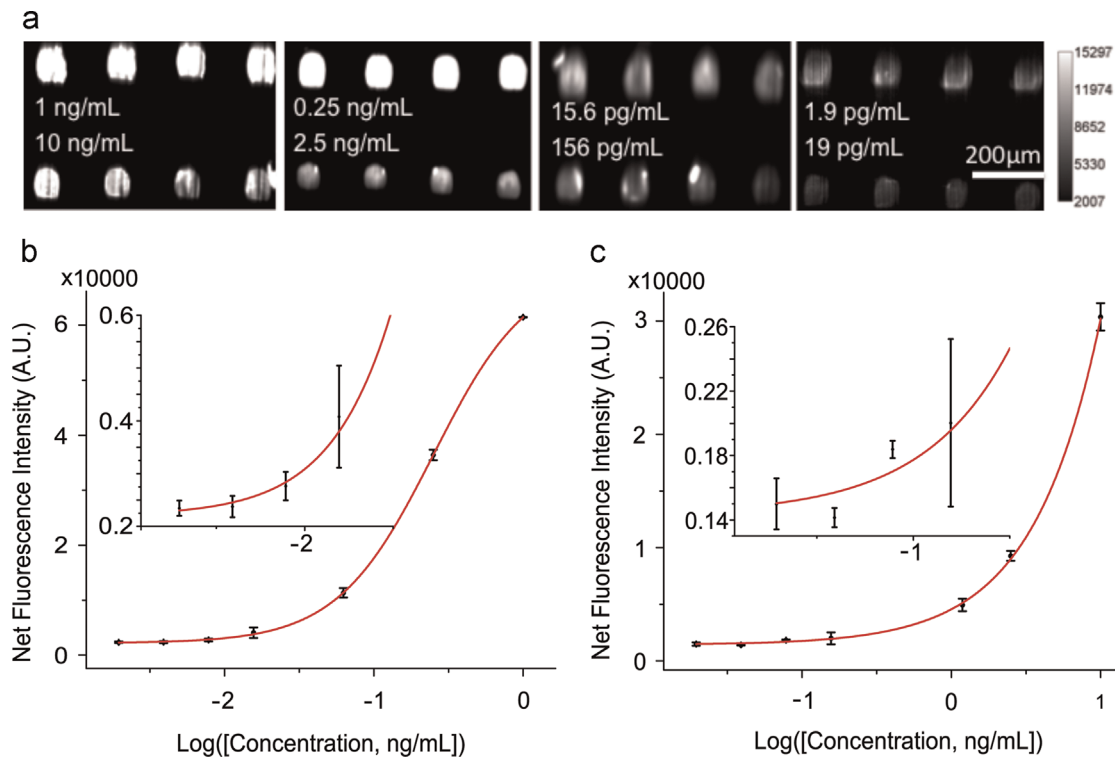


Fig. 6. (a) Representative fluorescence images of microspots on the PC at four sets of assayed concentrations. The first row contains TNF- α spots while the second row contains IL-3 spots. Standard curves for (b) TNF- α and (c) IL-3. LOD values for two cytokines TNF- α and IL-3 are 1.57 pg/mL and 17.96 pg/ml respectively. Error bars represent one standard deviation for all $N=4$ replicate spots.

the fluorescence intensity was enhanced by a factor of 26, which is similar to what was reported previously (Huang et al., 2011; Chaudhery et al., 2011). In general, we expect a PC embedded in the cartridge to perform identically to a PC in the “free” chip format, as the absorption and reflection of light by the thin glass cover are minimal.

3.3. Standard curves and limit of detection

The performance of the PC-embedded cartridge was studied in the context of a microspot-based fluorescent sandwich immunoassay. Seven concentrations of antigen mixtures were assayed by the PC microfluidic system as described in the previous sections. No leakage from the flanged tubes was observed for any of the performed experiments. The assay procedure was controlled by a computer with minimal human intervention. Fig. 6(a) shows representative fluorescence images of microspots at four sets of assayed concentrations. Compared with previously reported results obtained by manually handling the liquids (George et al., 2013), one obvious improvement realized by using the automatic system is the intensity uniformity within spots of the same cytokine. In order to quantitatively characterize how easily a spot can be distinguished from background noise, we defined signal to noise ratio (SNR) as the net signal divided by the standard deviation. A spot with SNR larger than 3 is regarded as detectable. Fig. 6(a) shows that all the cytokine spots were detectable over the 1.9 pg/mL–10 ng/mL range. For example, SNRs of the TNF- α spots and the IL-3 spots at the lowest concentrations are 50.0 and 78.3, respectively.

The signal intensities from each dilution in the concentration series were used to generate standard curves for both TNF- α (Fig. 6 (b)) and IL-3 ((c)) using Prism. The limit of detection (LOD) is defined as the concentration corresponding to the blank intensity (i.e. the intensity of the negative control spot of pbs buffer) plus 3 standard deviations from all assay spots. Negative controls

performed by exposing the capture antibodies to a casein sample resulted in no observable fluorescence signal above the background. Therefore, LOD values for the two cytokines TNF- α and IL-3 are 1.57 pg/ml and 17.96 pg/ml, respectively. While the LOD values are similar, the intensity uniformity within the spots is greatly improved compared to that obtained without the use of the microfluidic system. Coefficients of variance (CV) were calculated for the IL-3 spots at the lowest four concentrations in order to quantitatively compare the intensity uniformity (Fig. 7). It is obvious that CVs decreased dramatically by using the microfluidic system for sample handling. For example, the CV decreased from 44.91% to 10.54% for the microspots that were assayed at the lowest IL-3 concentration. the improvement in reproducibility is

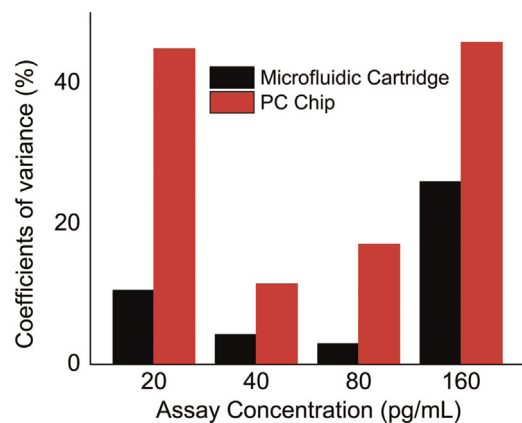


Fig. 7. Coefficients of variance (CVs) of the IL-3 spots at the lowest four concentrations (20 pg/mL, 40 pg/mL, 80 pg/mL and 160 pg/mL). Immunoassays for IL-3 were performed using PC-embedded microfluidic cartridges (black bars) and free PC chips (red bars). CVs decreased dramatically with the use of the microfluidic system for sample handling. (For interpretation of the references to color in this figure legend, the reader is referred to the web version of this article.)

attributed to three factors. First, the non-contact nature of the microfluidic method compared to manual injection removes the possibility of array damage through physical contact with pipette tips commonly used for injection/removal of assay liquids during sample introduction and washing steps. Second, no air bubbles are present with the automatic microfluidic system. Bubbles, when present over the assay during any step, can greatly decrease the incubation efficiency and result in variance from spot to spot. Because the liquid flow is continuous in the microfluidic system, no bubbles are introduced during the assay process. Using the manual approach, the small volume of the well and the pipette tip often results in generation of bubbles during liquid injection. Third, the wash steps are more thorough within the microfluidic system compared to the manual system. Note that we flowed ~ 3 ml wash buffer for ~ 30 s to remove the unbound molecules using the automatic microfluidic system while, with a manual assay, we only pipette ~ 15 μ l wash buffer three times into the well.

We directly compare our results to those obtained for the same analytes with commercially available approaches. We are especially concerned with the ability to achieve assay results at the point-of-care that are faster, more sensitive, and less invasive (in terms of sample volume required) than laboratory-based approaches. The traditional microplate ELISA remains one of the most popular assay platforms used for cancer biomarker analysis, which has no multiplexing capability with a detection limit of on the order of 10–50 pg/mL for an overnight sample incubation. Recently a multiplexed, sandwich assay has been developed which is based on a bead-based approach (Luminex). While the sensitivity of this bead-based approach approaches 2–10 pg/mL, it typically uses much larger volumes of serum (> 50 μ l) than available in a pin prick, requires an expensive non-automated detection instrument, provides limited multiplexing capability, and a more lengthy assay protocol than microarrays. The PC microfluidic approach, however, optimally use 10 μ l of sample to detect analytes at 1 pg/ml concentration, lacks assay cross-reactivity, and demonstrates the fastest binding kinetics (< 4 h incubation), while providing equivalent or lower limits of detection than bead-based assays due to the ability to wash away unbound material. Our new platform enables more rapid, high sensitivity detection and a simplified output that will be readily usable by a clinician.

4. Conclusion

In this work, we designed, fabricated, and demonstrated a microfluidic cartridge and assay automation system for performing multiplexed and high sensitivity fluorescent microarray sandwich assays that incorporate photonic crystal fluorescence enhancement. We have demonstrated 80 fM detection limits for two representative biomarkers (TNF- α and IL3) from a 10 μ l sample volume with small intensity variances across the replicate spots and detection limits that are identical to those obtained with the PC utilized in a highly manual assay protocol. The chip is held in a simple, inexpensive, and room-temperature-assembled cartridge that interfaces with an assay automation instrument. The assay instrument is comprised of a computer-controlled pressure manifold and three-way valve that automates the washing, labeling, and drying steps of the immunoassay. The cartridge interfaces with the assay automation instrument through a simple and leak-free press-fit seal that introduces no liquid dead volume. The described platform integrates many features that are required for a practical point-of-care immunoassay targeted at liquid-biopsy diagnostics: it is automatic and easy-to-use; it can perform multiple assays simultaneously; it requires only a small volume of test sample and reagents (~ 500 μ l); and high analytic sensitivity and

high selectivity are achieved. Moreover, the use of the automation system greatly reduces spot-to-spot coefficients of variability compared to manual handling.

Acknowledgement

This work was supported by Grants from the National Institutes of Health (GM086382A, R33CA177446, R01GM108584) and the National Science Foundation (CBET 07-54122). Any opinions, findings, conclusions, or recommendations expressed in this material are those of the authors and do not necessarily reflect the views of the National Institutes of Health or the National Science Foundation. The authors thank Scott McDonald and David Switzer at machine shop of ECE department for their help making the holding fixture.

References

- Au, A.K., Lee, W., Folch, A., 2014. Mail-order microfluidics: evaluation of stereolithography for the production of microfluidic devices. *Lab Chip* 14, 1294–1301.
- Bettegowda, C., Sausen, M., Leary, R.J., Kinde, I., Wang, Y., Agrawal, N., et al., 2014. Detection of circulating tumor DNA in early- and late-stage human malignancies. *Sci. Transl. Med.* 6, 224ra24.
- Block, I.D., Mathias, P.C., Ganesh, N., Jones, S.I., Dorvel, B.R., Chaudhery, V., et al., 2009. A detection instrument for enhanced-fluorescence and label-free imaging on photonic crystal surfaces. *Opt. Express* 17, 13222–13235.
- Borras, T.G.L., Tietz, J., 2010. Generic approach for the generation of stable humanized single-chain Fv fragments from rabbit monoclonal antibodies. *J. Biol. Chem.* 285, 12.
- Chaudhery, V., Lu, M., Huang, C., George, S., Cunningham, B., 2011. Photobleaching on photonic crystal enhanced fluorescence surfaces. *J. Fluoresc.* 21, 707–714 2011/03/01.
- Chaudhery, V., Lu, M., Huang, C.-S., Polans, J., Tan, R., Zangar, R.C., 2012. A line-scanning detection instrument for photonic crystal enhanced fluorescence. *Opt. Lett.* 37, 2565–2567.
- Choudhury, I.A., Shirley, S., 2010. Laser cutting of polymeric materials: an experimental investigation. *Opt. Laser Technol.* 42, 503–508 4//.
- Dawson, S.-J., Tsui, D.W.Y., Murtaza, M., Biggs, H., Rueda, O.M., Chin, S.-F., et al., 2013. Analysis of circulating tumor DNA to monitor metastatic breast cancer. *N. Engl. J. Med.* 368, 1199–1209.
- Debnath, M., 2010. *Molecular Diagnostics: Promises and Possibilities*. Springer Science+Business Media, pp. 503–513.
- Diamandis, E.P., Borgono, C.A., Scorilas, A., Yousef, G.M., Harbeck, N., Dorn, J., et al., 2003. Immunofluorometric quantification of human kallikrein 5 expression in ovarian cancer cytosols and its association with unfavorable patient prognosis. *Tumor Biol.* 24, 299–309.
- Diamandis, E.P., Scorilas, A., Fracchioli, S., van Gramberen, M., de Bruijn, H., Henrik, A., et al., 2003. Human kallikrein 6 (hK6): a new potential serum biomarker for diagnosis and prognosis of ovarian carcinoma. *J. Clin. Oncol.* 21, 1035–1043 15.
- Dorvel, B., Reddy, B., Block, I., Mathias, P., Clare, S.E., Cunningham, B., et al., 2009. Vapor-phase deposition of monofunctional alkoxysilanes for sub-nanometer-level biointerfacing on silicon oxide surfaces. *Adv. Funct. Mater.* 20, 87–95.
- Eltawahni, H.A., Hagino, M., Benyounis, K.Y., Inoue, T., Olabi, A.G., 2012. Effect of CO₂ laser cutting process parameters on edge quality and operating cost of AISI316L. *Opt. Laser Technol.* 44, 1068–1082 6//.
- Fan, R., Vermesh, O., Srivastava, A., Yen, B.K.H., Qin, L.D., Ahmad, H., et al., 2008. Integrated barcode chips for rapid, multiplexed analysis of proteins in microliter quantities of blood. *Nat. Biotechnol.* 26, 1373–1378.
- Ganesh, N., Zhang, W., Mathias, P.C., Chow, E., Soares, J.A.N.T., Malyarchuk, V., et al., 2007. Enhanced fluorescence emission from quantum dots on a photonic crystal surface. *Nat. Nano* 2, 515–520 08//print.
- George, S., Chaudhery, V., Lu, M., Takagi, M., Amro, N., Pokhriyal, A., et al., 2013. Sensitive detection of protein and miRNA cancer biomarkers using silicon-based photonic crystals and a resonance coupling laser scanning platform. *Lab Chip* 13, 4053–4064.
- Gonzalez, R.M., Daly, D.S., Tan, R., Marks, J.R., Zangar, R.C., 2015. Plasma biomarker profiles differ depending on breast cancer subtype but RANTES in consistently increased. *Cancer Epidemiol. Biomark. Prev.* 20, 1543–1551.
- Huang, C.-S., George, S., Lu, M., Chaudhery, V., Tan, R., Zangar, R.C., et al., 2011. Application of photonic crystal enhanced fluorescence to cancer biomarker microarrays. *Anal. Chem.* 83, 1425–1430 2011/02/15.
- Jain, K.K., 2010. *The Handbook of Biomarkers: Springer Science+Business Media. Humana Press.*
- Jeffrey, S.S., 2008. Cancer biomarker profiling with microRNAs. *Nat. Biotechnol.* 26, 400–401 04//print.
- Khoo, S.K., Petillo, D., Kang, U.J., Resau, J.H., Berryhill, B., Linder, J., et al., 2012. Plasma-based circulating microRNA biomarkers for Parkinson's disease. *J.*

- Parkinson's Dis. 2, 321–331 01/01/.
- Luo, L.Y., Katsaros, D., Scorilas, A., Fracchioli, S., Bellino, R., van Gramberen, M., et al., 2003. The serum concentration of human kallikrein 10 represents a novel biomarker for ovarian cancer diagnosis and prognosis. *Cancer Res.* 63, 807–811.
- Maurya, P., Meleady, P., Dowling, P., Clynes, M., 2007. Proteomic approaches for serum biomarker discovery in cancer. *Anticancer Res.* 27, 1247–1255.
- Melchels, F.P.W., Feijen, J., Grijpma, D.W., 2010. A review on stereolithography and its applications in biomedical engineering. *Biomaterials* 31, 6121–6130 8//.
- Nam, M.J., Madoz-Gurpide, J., Wang, H., Lescure, P., Schmalbach, C.E., Zhao, R., et al., 2003. Molecular profiling of the immune response in colon cancer using protein microarrays: occurrence of autoantibodies to ubiquitin C-terminal hydrolase L3. *Proteomics* 3, 2108–2115.
- Neagu, M., Constantin, C., Tanase, C., Boda, D., 2011. Patented biomarker panels in early detection of cancer. *Recent Pat. Biomark.* 1, 10–24.
- Newman, A.M., Bratman, S.V., To, J., Wynne, J.F., Eclow, N.C.W., Modlin, L.A., 2014. An ultrasensitive method for quantitating circulating tumor DNA with broad patient coverage. *Nat. Med.* 20 (5), 548–554.
- Nie, J., Liang, Y., Zhang, Y., Le, S., Li, D., Zhang, S., 2013. One-step patterning of hollow microstructures in paper by laser cutting to create microfluidic analytical devices. *Analyst* 138, 671–676.
- Patz, E.F., Campa, M.J., Gottlin, E.B., Kusmartseva, I., Guan, X.R., Herndon, J.E., 2007. Panel of serum biomarkers for the diagnosis of lung cancer. *J. Clin. Oncol.* 25, 5578–5583.
- Pokhriyal, A., Lu, M., Chaudhery, V., Huang, C.-S., Schulz, S., Cunningham, B.T., 2010. Photonic crystal enhanced fluorescence using a quartz substrate to reduce limits of detection. *Opt. Express* 18, 24793–24808 2010/11/22.
- Robinson, W.H., DiGennaro, C., Hueber, W., Haab, B.B., Kamachi, M., Dean, E.J., et al., 2002. Autoantigen microarrays for multiplex characterization of autoantibody responses. *Nat. Med.* 8, 295–301.
- Sita-Lumsden, A., Dart, D.A., Waxman, J., Bevan, C.L., 2013. Circulating microRNAs as potential new biomarkers for prostate cancer. *Br. J. Cancer* 108, 1925–1930 05/28/print.
- Tannapfel, A., Anhalt, K., Hausermann, P., Sommerer, F., Benicke, M., Uhlmann, D., et al., 2003. Identification of novel proteins associated with hepatocellular carcinomas using protein microarrays. *J. Pathol.* 201, 238–249.
- Vasan, R.S., 2006. Biomarkers of cardiovascular disease—molecular basis and practical considerations. *Circulation* 113, 2335–2362.
- Wang, T.J., Gona, P., Larson, M.G., Tofler, G.H., Levy, D., Newton-Cheh, C., et al., 2006. Multiple biomarkers for the prediction of first major cardiovascular events and death. *N. Engl. J. Med.* 355, 2631–2639.
- Ward, D.G., Suggett, N., Cheng, Y., Wei, W., Johnson, H., Billingham, L.J., et al., 2006. Identification of serum biomarkers for colon cancer by proteomic analysis. *Br. J. Cancer* 94, 1898–1905.
- Wilhelm, E., Neumann, C., Duttenhofer, T., Pires, L., Rapp, B.E., 2013. Connecting microfluidic chips using a chemically inert, reversible, multichannel chip-to-world-interface. *Lab Chip* 13, 4343–4351.
- Wong, J., Sibani, S., Lokko, N.N., LaBaer, J., Anderson, K.S., 2009. Rapid detection of antibodies in sera using multiplexed self-assembling bead arrays. *J. Immunol. Methods* 350, 171–182.
- Zangar, R.C., Varnum, S.M., Bollinger, N., 2005. Studying cellular processes and detecting disease with protein microarrays. *Drug Metab. Rev.* 37, 473–487.
- Zhang, A.P., Qu, X., Soman, P., Hribar, K.C., Lee, J.W., Chen, S., et al., 2012. Rapid fabrication of complex 3D extracellular microenvironments by dynamic optical projection stereolithography. *Adv. Mater.* 24, 4266–4270.
- Zhang, Z., Bast, R.C., Yu, Y.H., Li, J.N., Sokoll, L.J., Rai, A.J., et al., 2004. Three biomarkers identified from serum proteomic analysis for the detection of early stage ovarian cancer. *Cancer Res.* 64, 5882–5890.
- Zhu, H., Klemic, J.F., Chang, S., Bertone, P., Casamayor, A., Klemic, K.G., et al., 2000. Analysis of yeast protein kinases using protein chips. *Nat. Genet.* 26, 283–290.